Supplemental Figure 1

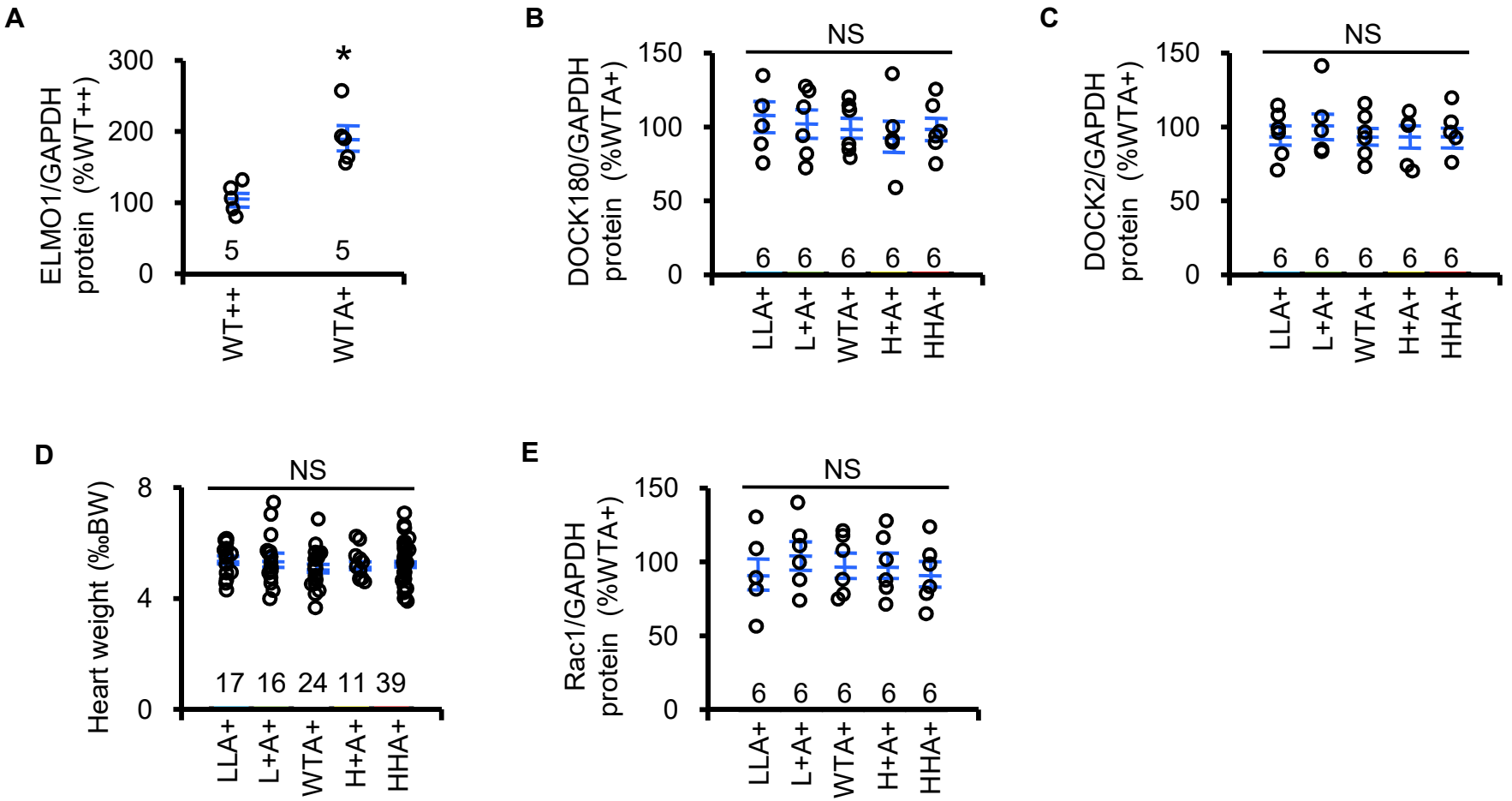

Supplemental Figure 1. ELMO1 and related protein levels. The number of animals studied is shown in each figure. Comparisons were done with one-way ANOVA. *, $P< 0.05$ vs. WT++ mice. NS, not significantly different among the 5 groups. **(A)** Relative ELMO1 protein levels in non-diabetic WT (WT++) and diabetic WT Akita (WTA+) hearts at age 16 weeks. **(B)** Relative dedicator of cytokinesis (DOCK) 180 protein levels, **(C)** relative DOCK2 protein levels, and **(D)** Heart weight normalized by body weight (BW), and **(E)** relative Rac1 protein levels in Akita mice with 5 graded expressions of *Elmo1* at age 16 weeks.

Supplemental Figure 2

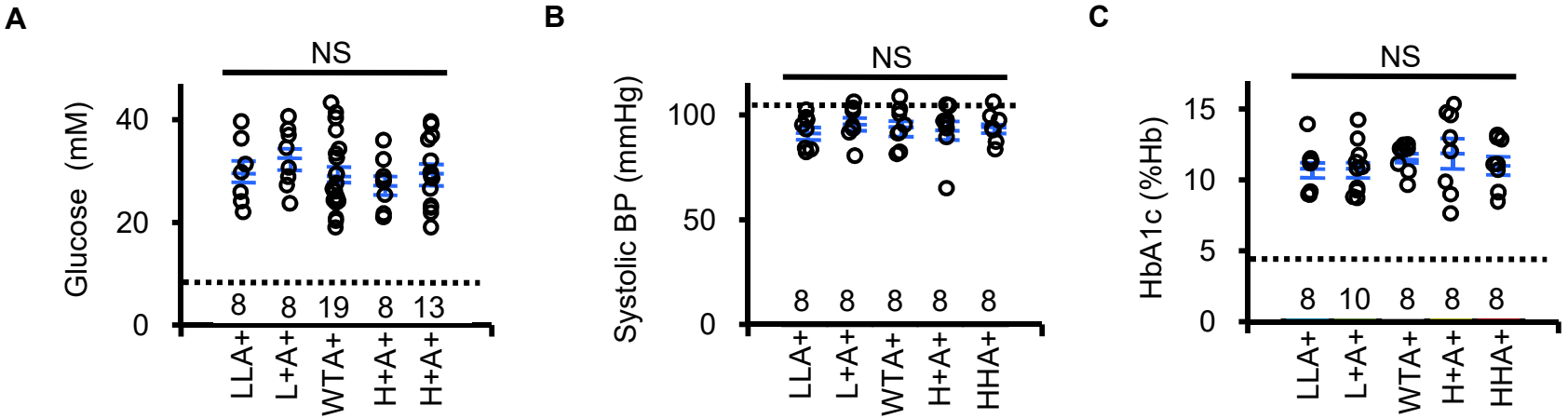

Supplemental Figure 2. Physiological parameters in Akita mice with 5 graded expressions of *Elmo1* at age 16 weeks. Number of animals used are indicated in each figure. Dotted lines indicate non-diabetic WT levels. Comparisons were done with one-way ANOVA including the additional data set. NS, not significantly different among the 5 groups. **(A)** Plasma glucose. **(B)** Systolic blood pressure (BP). **(C)** Hemoglobin A1c (HbA1c) in the blood.

Supplemental Figure 3

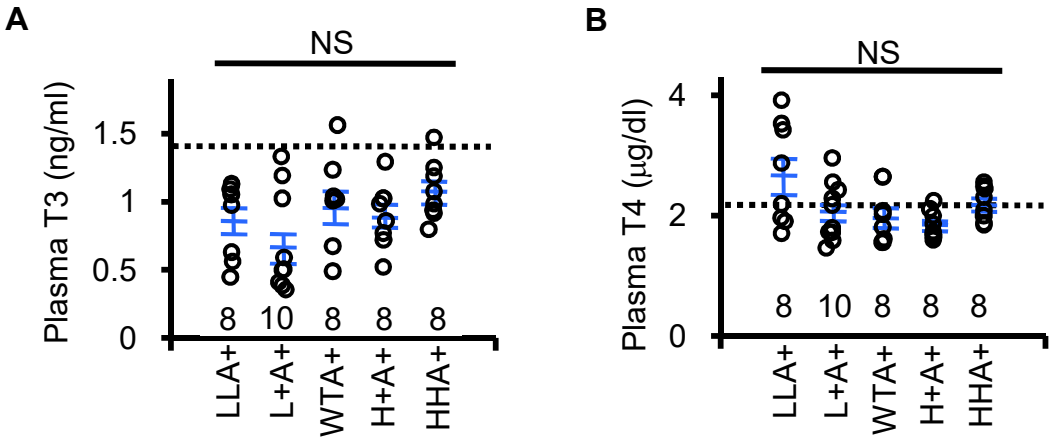

Supplemental Figure 3. Thyroid function in Akita mice with 5 graded expressions of *Elmo1* at age 16 weeks. Error bars are means ± SEM. Number of animals used are indicated in each figure. Dotted lines indicate non-diabetic WT levels. Comparisons were done with one-way ANOVA. NS, not significantly different among the 5 groups. **(A)** Plasma triiodothyronine (T3) levels. **(B)** Plasma thyroxine (T4) levels.

Supplemental Figure 4

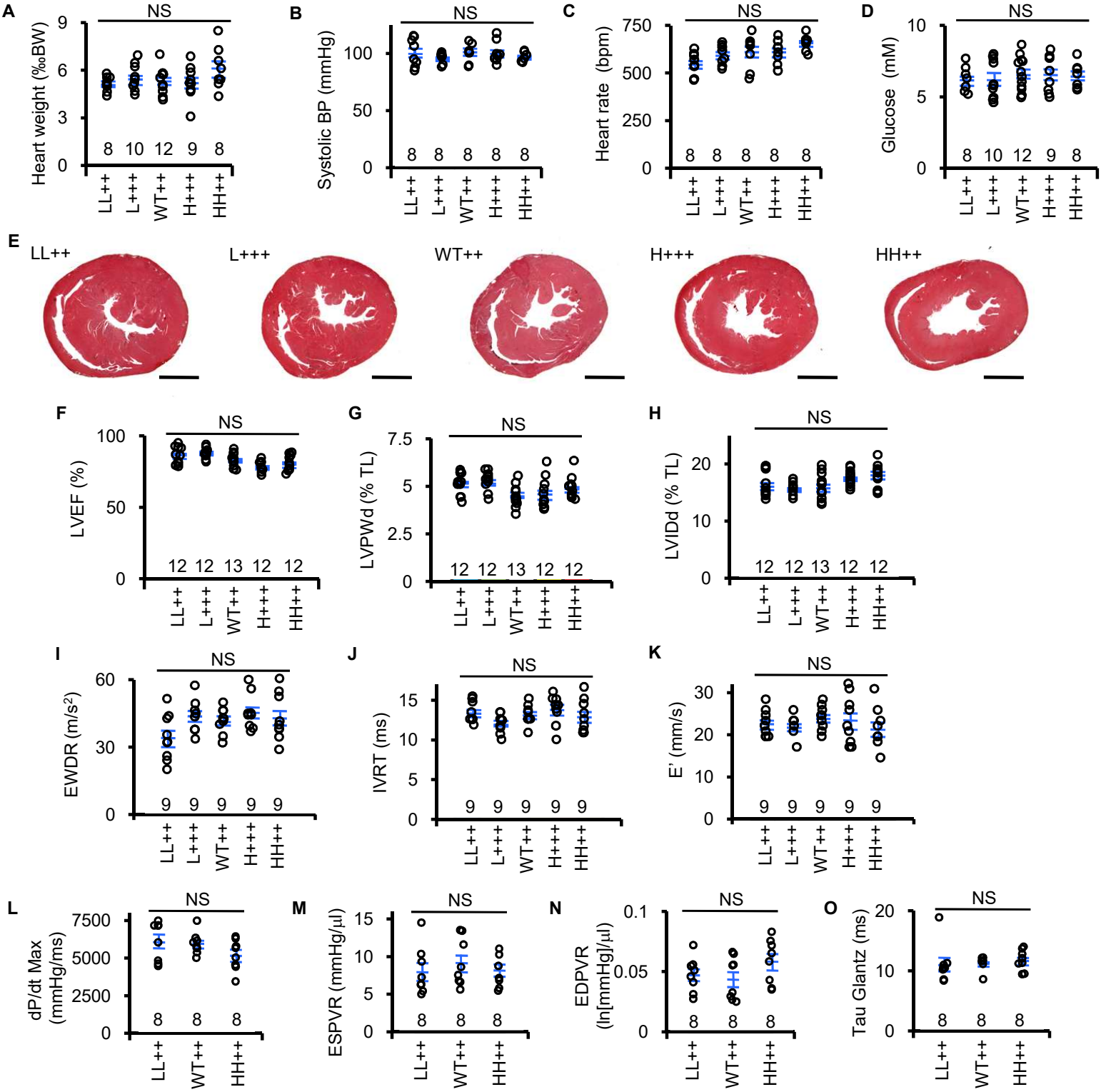

Supplemental Figure 4. Baseline values, histology, and cardiac functions with echocardiography and pressure-volume (PV) loop analysis in the non-diabetic mice with 5 graded expressions of *Elmo1* at age 16 weeks. The number of animals studied is shown in each figure. Comparisons were done with one-way ANOVA including the additional data set. NS, not significantly different among the 5 groups. **(A)** Heart weight normalized by body weight. **(B)** Systolic blood pressure (BP). **(C)** Heart rate. **(D)** Plasma glucose. **(E)** AZAN trichrome staining of the heart. Scale bar = 1 mm. **(F)** Ejection fraction of the left ventricles (LVEF). **(G)** Thickness of the left ventricular posterior wall in diastole (LVPWd). **(H)** Internal diameter of the left ventricle in diastole (LVIDd). **(I)** E-wave deceleration rate (EWDR) of the mitral flow. **(J)** The isovolumic relaxation time (IVRT) of the left ventricle. **(K)** Early tissue Doppler velocity (E'). **(L)** dP/dt Max. **(M)** End-systolic pressure-volume relationship (ESPVR). **(N)** End-diastolic pressure-volume relationship (EDPVR). **(O)** Tau Glantz.

Supplemental Figure 5

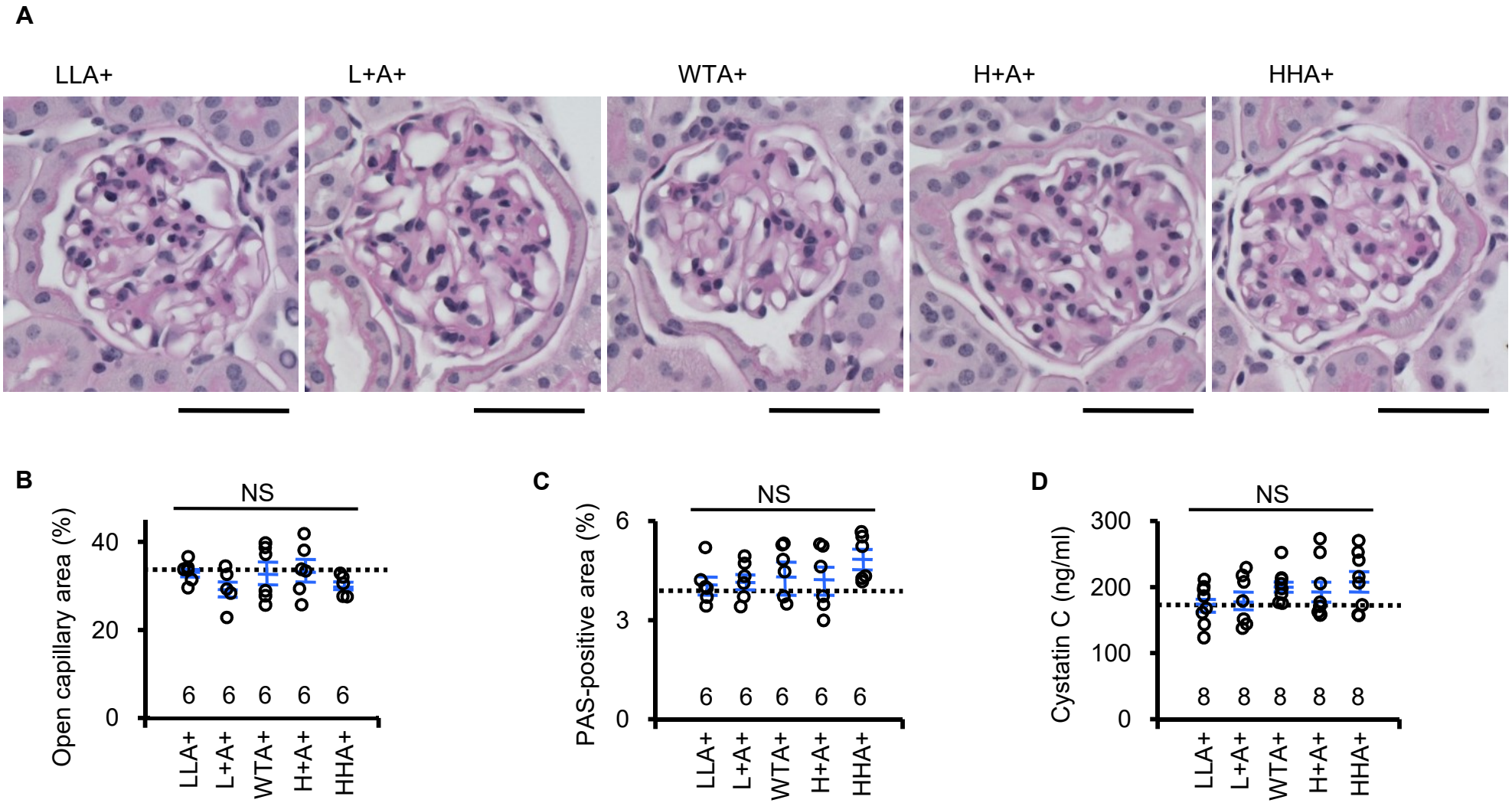

Supplemental Figure 5. Renal histology and function in Akita mice with 5 graded expressions of *Elmo1* at age 16 weeks. Dotted line indicates non-diabetic WT levels. The number of animals studied is shown in each figure. Twenty glomeruli were analyzed in each animal for histology. Comparisons were done with one-way ANOVA including the additional data set. NS, not significantly different among the 5 groups. **(A)** Periodic acid-Schiff (PAS) staining with hematoxylin counter stain of the glomerulus. Scale bar = 50 µm. **(B)** Open capillary area. **(C)** PAS-positive area. **(D)** Plasma cystatin C levels.

Supplemental Figure 6

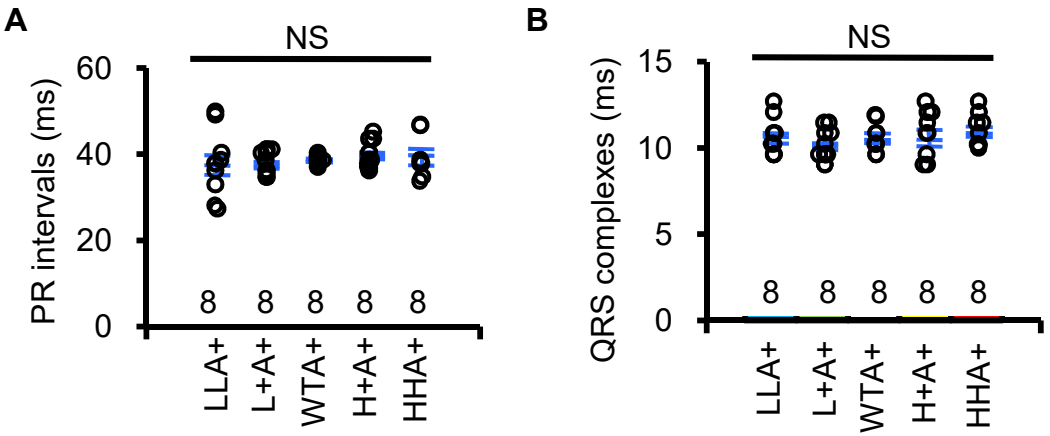

Supplemental Figure 6. Parameters in the electrocardiogram. Eight mice in each group were examined. NS, not significantly different by one-way ANOVA. **(A)** PR intervals. **(B)** QRS complexes.

Supplemental Figure 7

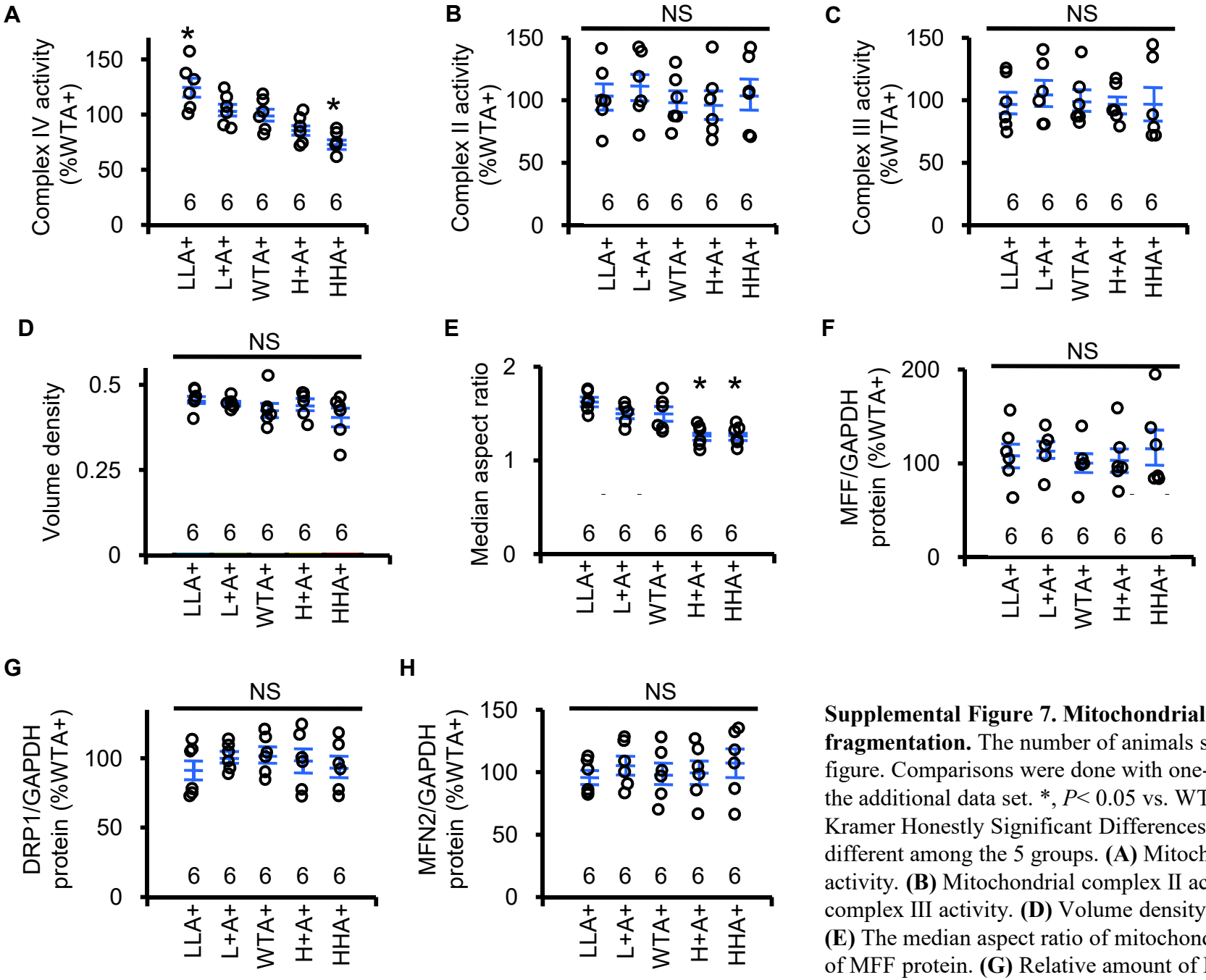

Supplemental Figure 7. Mitochondrial dysfunction and fragmentation. The number of animals studied is shown in each figure. Comparisons were done with one-way ANOVA including the additional data set. *, $P< 0.05$ vs. WTA+ mice by Tukey-Kramer Honestly Significant Differences test. NS, not significantly different among the 5 groups. **(A)** Mitochondrial complex IV activity. **(B)** Mitochondrial complex II activity. **(C)** Mitochondrial complex III activity. **(D)** Volume density of the mitochondria. **(E)** The median aspect ratio of mitochondria. **(F)** Relative amount of MFF protein. **(G)** Relative amount of DRP1 protein. **(H)** Relative amount of MFN2 protein.

Supplemental Figure 8

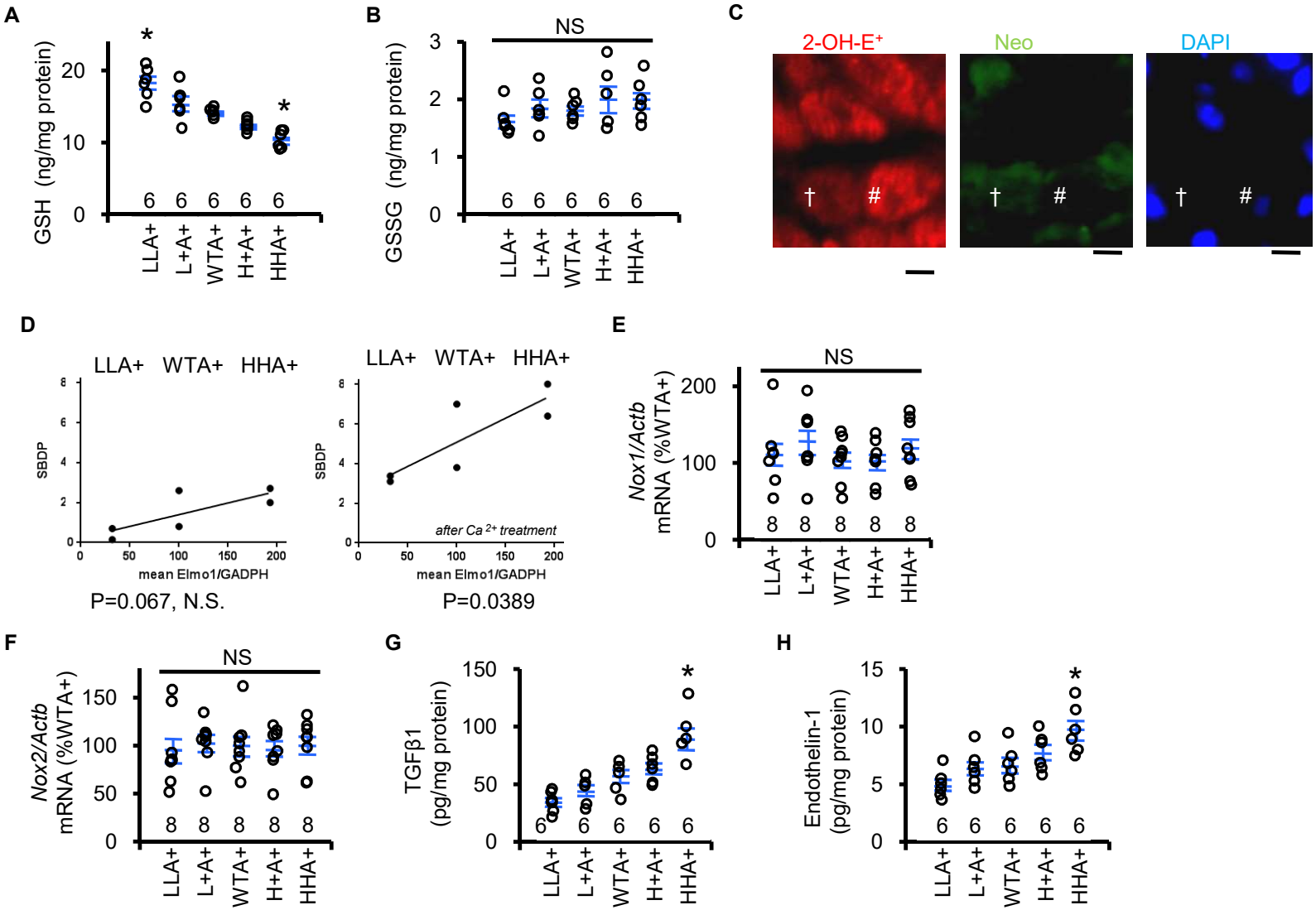

Supplemental Figure 8. Oxidative stress-related markers in the cardiac tissues. The number of animals studied is shown in each figure. Comparisons were done with one-way ANOVA including the additional data set. *, $P< 0.05$ vs. WTA+ mice by Tukey-Kramer Honestly Significant Differences test. NS, not significantly different among the 5 groups. **(A)** GSH content in the five groups of mice, six mice in each group. **(B)** GSSG content in the five groups of mice, six mice in each group. **(C)** Individual fluorescence for 2-OH-E$^+$ fluorescence (Red), Neomycin phosphotransferase II (Neo) immunoreactivity (Green), and nuclei attaining with DAPI (Blue) in the heart of the *Elmo1*$^{L/+}$*Myh6-cre/Esr1Ins2*$^{Akita/+}$ mice intraperitoneally injected with low dose tamoxifen (20 mg/kg, 2 days). Tissue was chimeric with Neo-positive *Elmo1*$^{L/+}$ cardiomyocytes and Neo-negative *Elmo1*$^{H/+}$ cardiomyocytes. The merged image is presented in Figure 5D of the main text. The Neo-positive *Elmo1*$^{L/+}$ cardiomyocyte (†) has a lower 2-OH-E$^+$ fluorescence than the Neo-negative *Elmo1*$^{H/+}$ cardiomyocyte (#). Scale bar = 10 μm. **(D)** Densitometric measures of the spectrin breakdown products (SBDP) before and after Ca^{2+} treatment were plotted on the left and the right, respectively. Values are expressed as % of αII-spectrin and plotted against mean *Elmo1* gene expression levels of LLA+ (30 %), WTA+ (100 %) and HHA+ (200 %). Two mice in each group. **(E)** mRNA levels of *Nox1*. **(F)** mRNA levels of *Nox2*. Amount of mRNA in each sample was normalized by mRNA of *Actb* (β-actin) and expressed relative to the mean values of WT A/+ as 100 %. **(G)** Protein levels of TGFβ1. **(H)** Protein levels of endothelin-1.

Supplemental Figure 9

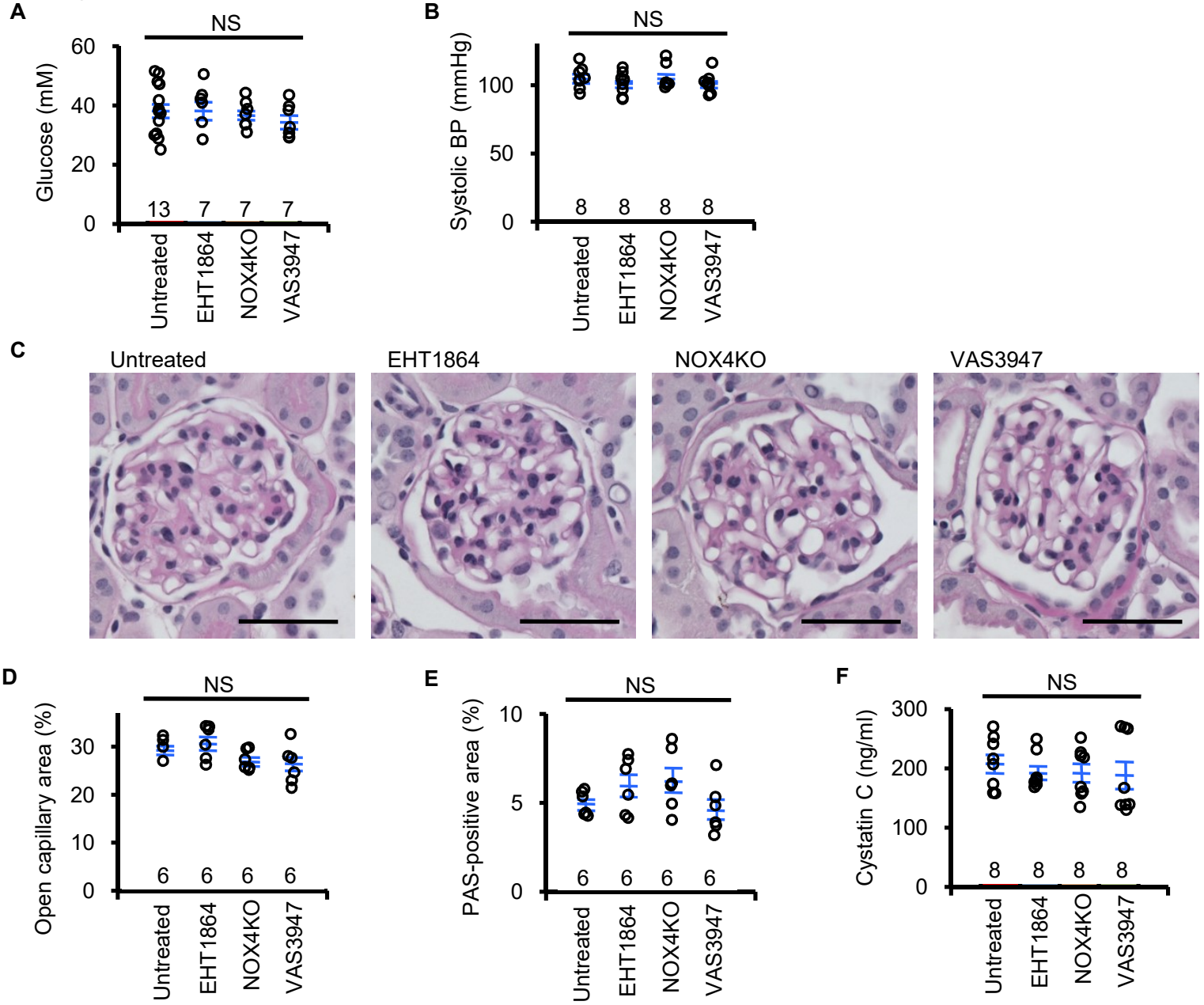

Supplemental Figure 9. Effects of EHT1864 (a pan-Rac inhibitor) and VAS3947 (a pan NADPH oxidase inhibitor) and disruption of *Nox4* (NOX4KO) in the HHA+ mice. Data of the untreated HHA+ mice are the same as those in the Supplemental Figure 4B, D and Supplemental Figure 5A-D. The number of animals studied is shown in each figure. Twenty glomeruli were analyzed in each animal for histology. Comparisons were done with one-way ANOVA including the additional data set. NS, not significantly different among the 4 groups. **(A)** Plasma glucose. **(B)** Systolic blood pressure (BP). **(C)** Periodic acid-Schiff (PAS) staining with hematoxylin counter stain of the glomerulus. Scale bar = 50 µm. **(D)** Open capillary area. **(E)** PAS-positive area. **(F)** Plasma cystatin C levels.

Supplemental Figure 10

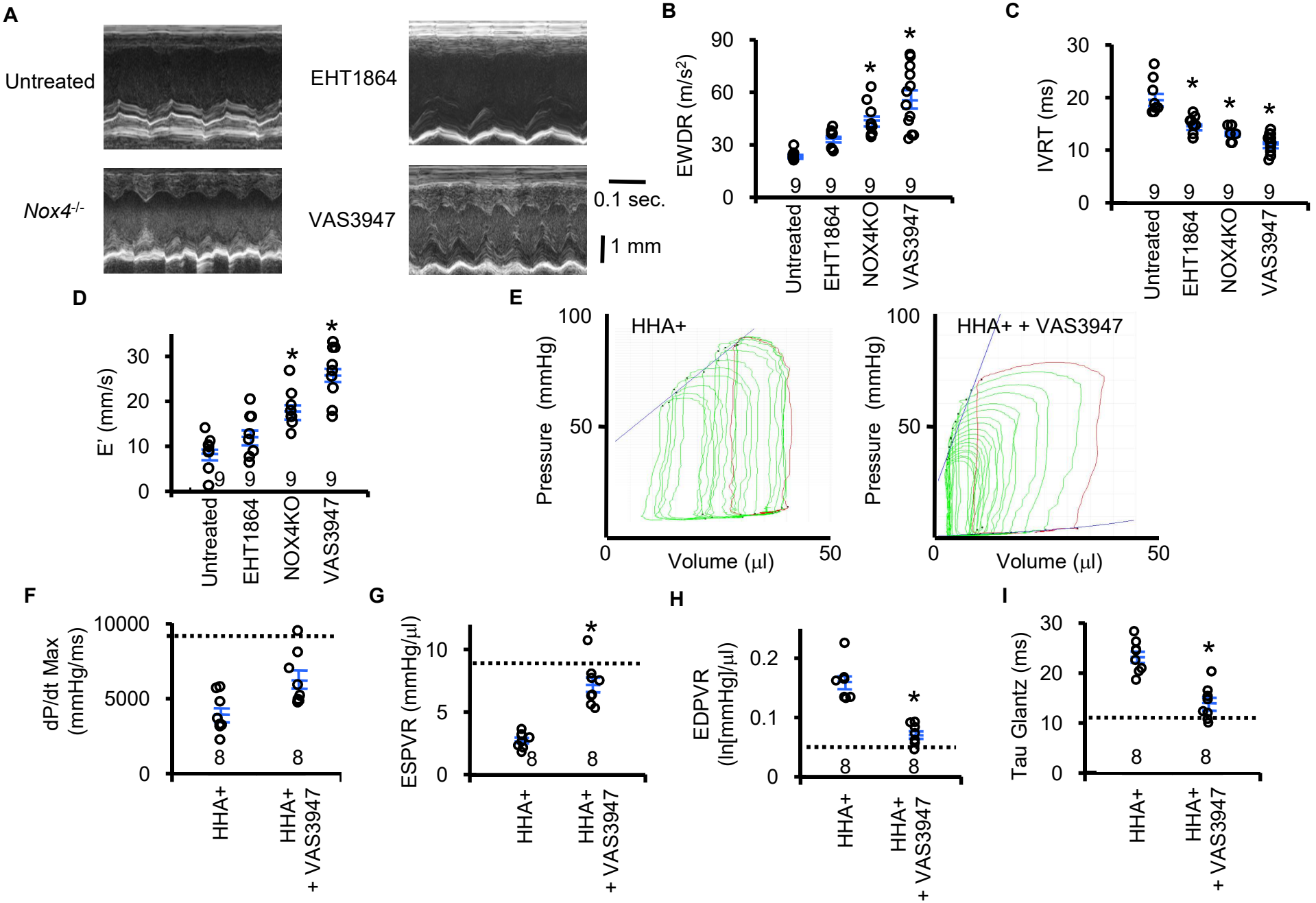

Supplemental Figure 10. Echocardiography and pressure-volume loop study in the HHA+ mice subjected to the 4-week treatment with VAS3947 at age 16 weeks. Data of the untreated HHA+ mice are the same as those in the Figure 2A, F-M of the main text. Dotted lines indicate non-diabetic WT levels. The number of animals studied is shown in each figure. Comparisons were done with one-way ANOVA including the additional data set. *, $P< 0.05$ vs. untreated HHA+ mice by Tukey-Kramer Honestly Significant Differences test. **(A)** Representative M-mode echocardiography of the HHA+ mice treated with vehicle, EHT1864 or VAS3947, and of Nox4-null HHA+ mice. **(B)** E-wave deceleration rate (EWDR) of the mitral flow. **(C)** The isovolumic relaxation time (IVRT) of the left ventricle **(D)** Early tissue Doppler velocity (E'). **(E)** Representativepressure-volume loops. **(F)** dP/dt Max. **(G)** End-systolic pressure-volume relationship (ESPVR). **(H)** End-diastolic pressure-volume relationship (EDPVR). **(I)** Tau Glantz.

Supplemental Figure 11

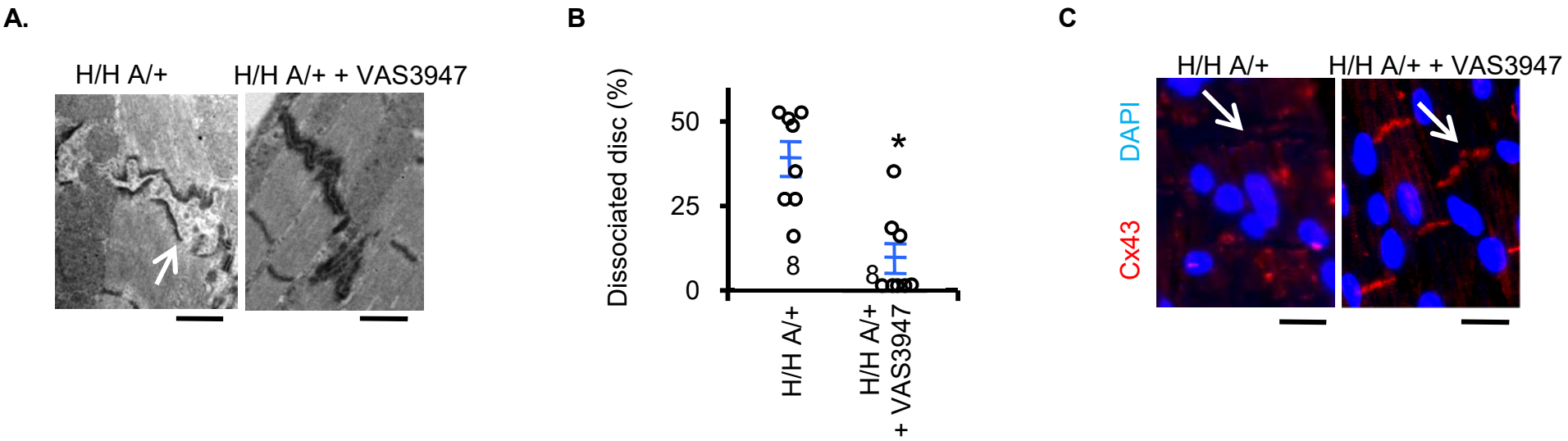

Supplemental Figure 11. Dissociation of the intercalated disc of heart muscle cells in the HHA+ mice treated with VAS3947. Data for the treated mice are presented together with those of HHA+ mice presented in the Figure 3A-C of the main text for comparison. The number of animals studied is shown in each figure. Comparisons were done with one-way ANOVA including the additional data set. *, $P< 0.05$ vs. untreated HHA+ mice by Tukey-Kramer Honestly Significant Differences test. **(A)** Representative images of the intercalated disc in the heart by the transmission electron microscopy (TEM). Arrows indicate the dissociation of intercalated disc. Scale bar = 1 μm. **(B)** Frequency of the dissociation of intercalated disc. Percentage of discs with dissociated gap junctions per at least 30 discs. *$P< 0.05$ vs. HHA+ by one-way ANOVA. **(C)** Representative images for the immunofluorescence for connexin 43 (Cx43). The immunoreactivity for connexin43 was diminished in the intercalated discs in the HHA+ heart, which was restored by VAS3947. Arrows indicate intercalated discs. Scale bar = 10 μm.

Supplemental Figure 12

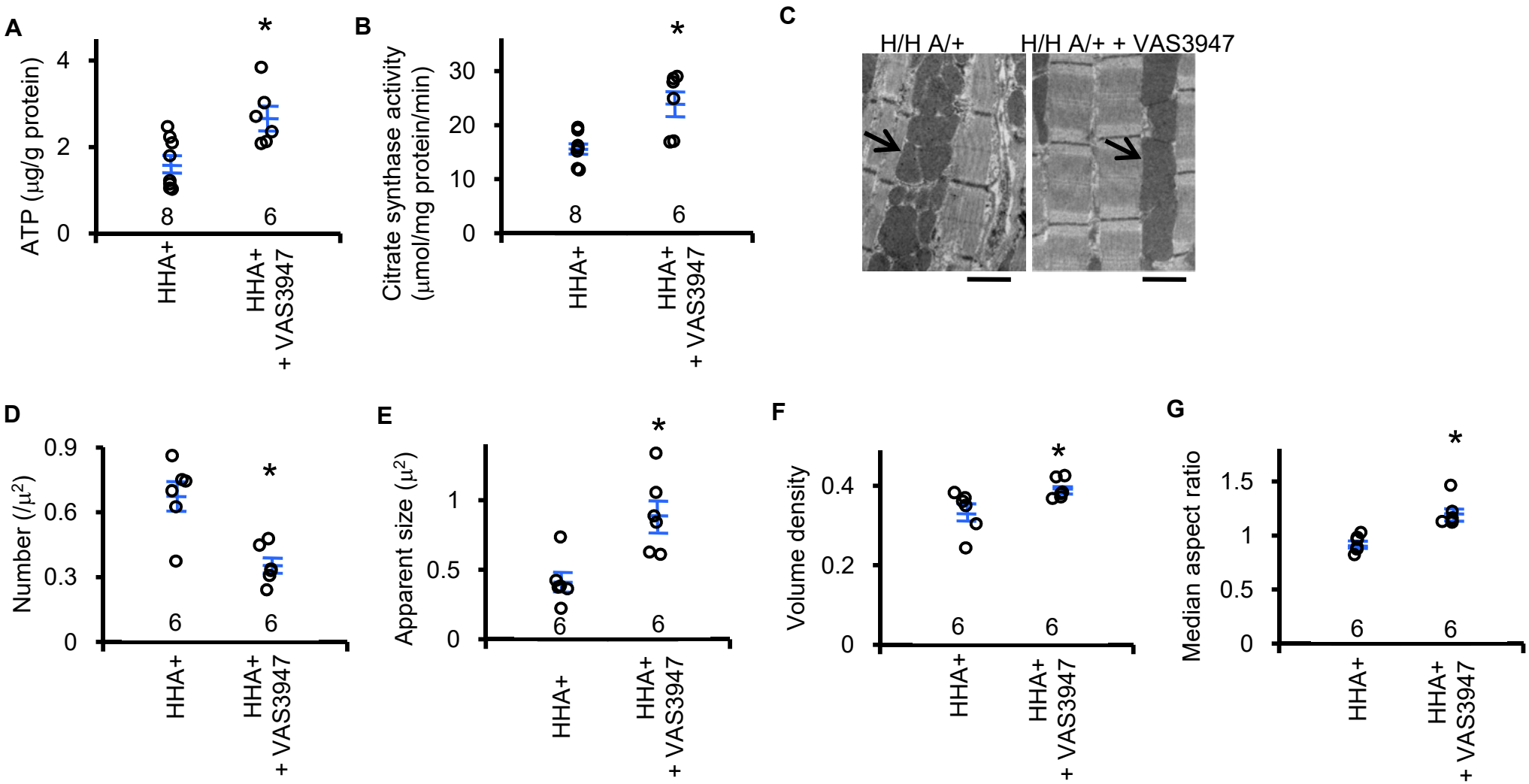

Supplemental Figure 12. Mitochondrial dysfunction and fragmentation in the heart of HHA+ mice treated with VAS3947. The results from the six treated mice are presented together with those of HHA+ mice presented in the Figure 4A, B, E-G and Supplemental Figure 7D, E of the main text for comparison. Comparisons were done with one-way ANOVA including the additional data set. *, $P< 0.05$ vs. untreated HHA+ mice by Tukey-Kramer Honestly Significant Differences test. **(A)** ATP content. **(B)** Citrate synthase activity. **(C)** Representative TEM images of the mitochondria. The fragmentation was frequently observed in the Akita mice with high expression of *Elmo1,* which was restored by VAS3947. Arrows indicate mitochondria. Scale bar = 1 μm. **(D)** The number of the mitochondria. **(E)** Apparent sizes of the mitochondria. **(F)** Volume density of the mitochondria. **(G)** The median aspect ratio of mitochondria.

Supplemental Figure 13

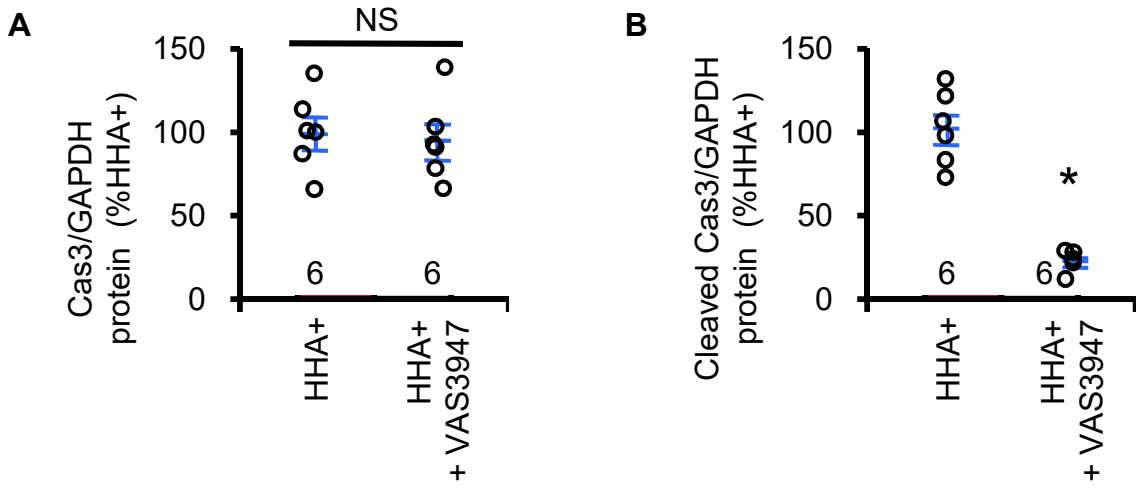

Supplemental Figure 13. Effects of VAS3947 on cleaved caspase 3 levels in the cardiac tissue of the HHA+ mice. The number of animals studied is shown in each figure. *, $P < 0.05$ vs. untreated HHA+ mice by one-way ANOVA. NS, not significantly different between the 2 groups. **(A)** Relative amount of total caspase 3. **(B)** Relative amount of cleaved caspase 3.

Supplemental Figure 14

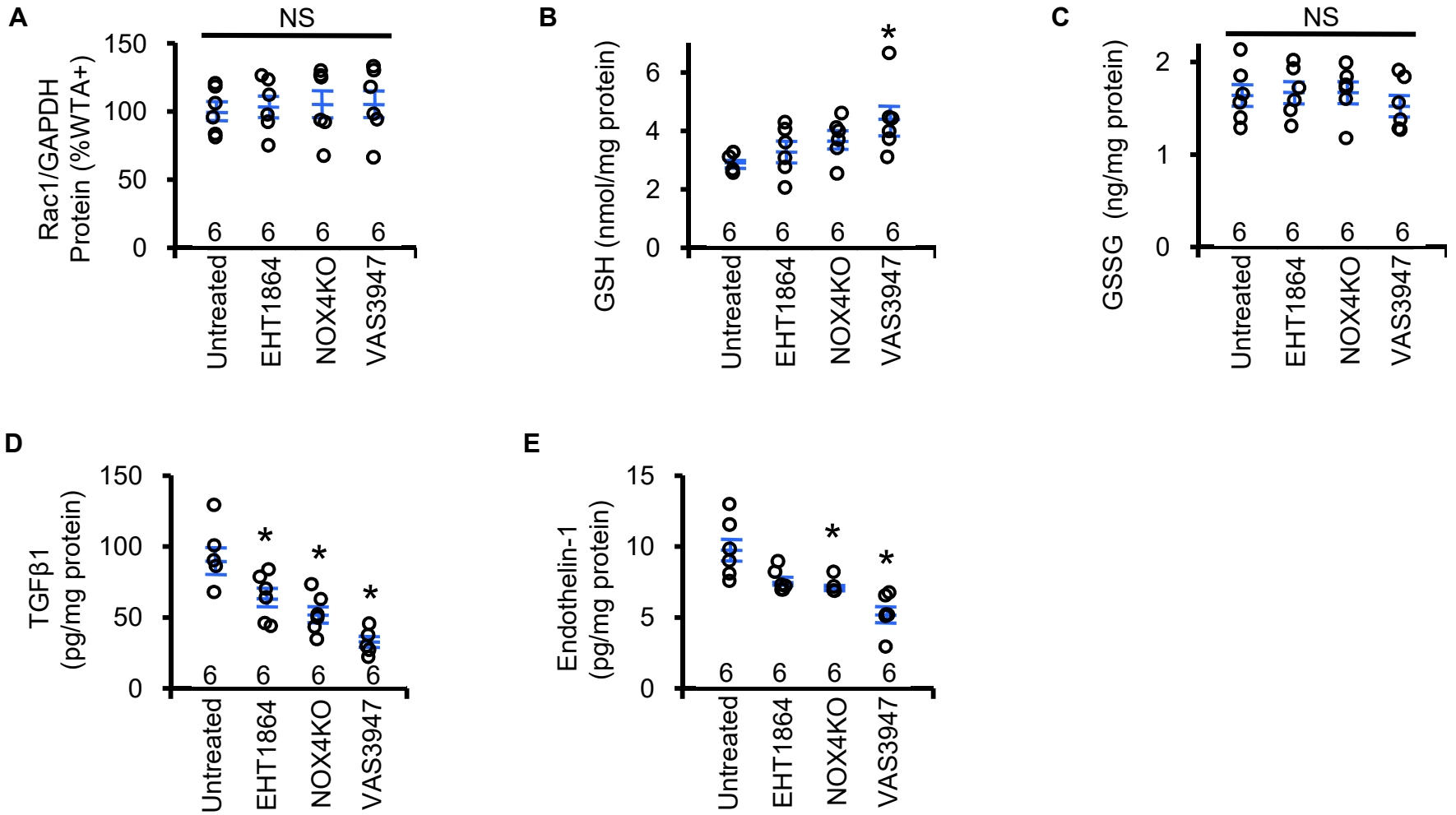

Supplemental Figure 14. Effects of EHT1864 and VAS3947 and disruption of *Nox4* (NOX4KO) on glutathione and protein levels in the cardiac tissue of the HHA+ mice. Data of the untreated HHA+ mice were taken from the previous experiments. The number of animals studied is shown in each figure. Comparisons were done with one-way ANOVA including the additional data set. *, $P< 0.05$ vs. untreated HHA+ mice by Tukey-Kramer Honestly Significant Differences test. NS, not significantly different among the 4 groups. **(A)** Total Rac protein. **(B)** GSH content. **(C)** GSSG content. **(D)** Protein levels of TGFβ1. **(E)** Protein levels of endothelin-1.

Supplemental Figure 15

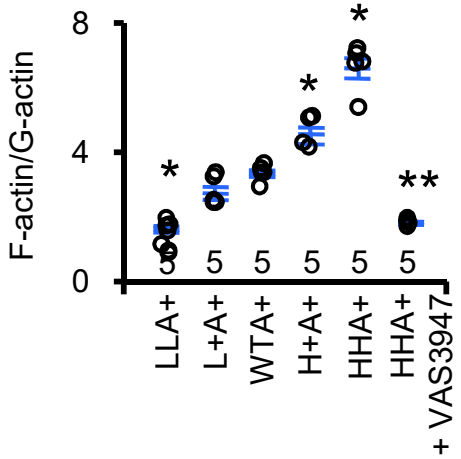

Supplemental Figure 15. Filamentous (F-) and globular (G-) actin protein levels in diabetic hearts at age 16 weeks. F-actin/G-actin ratios in the diabetic heart having 5 ELMO1 genetic levels and the HHA+ heart treated with VAS3947. The number of animals studied is shown in each figure. Comparisons were done with one-way ANOVA. *, $P< 0.05$ vs WTA+ mice; **, $P< 0.05$ vs. untreated HHA+ mice by Tukey-Kramer Honestly Significant Differences test.

Supplemental Figure 16

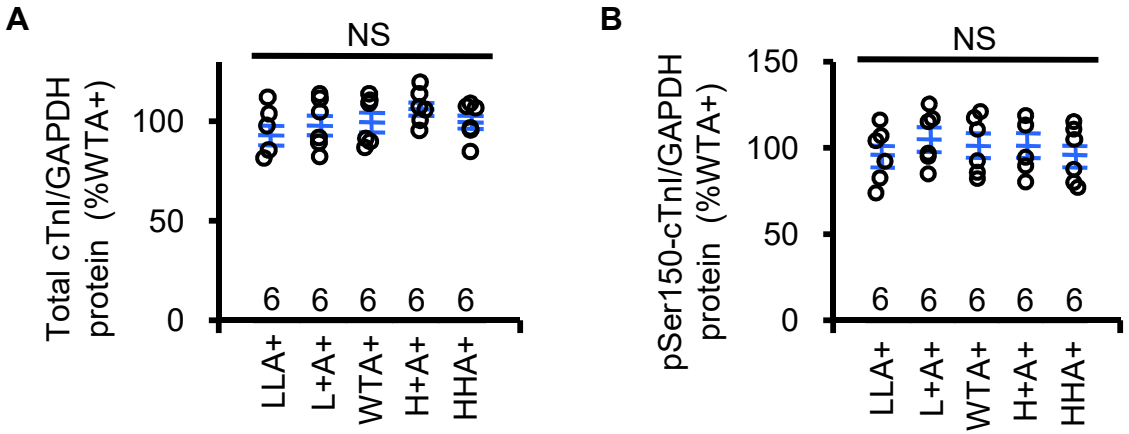

Supplemental Figure 16. Immunoblots for total and Ser150-phosphorylated cardiac troponin I (cTnI) using the whole heart lysate of Akita mice with graded ELMO1 expression. The number of animals studied is shown in each figure. Comparisons were done with one-way ANOVA. NS, not significantly different among the 5 groups. No difference was observed in **(A)** the total amount and in **(B)** Ser150-phosphorylated **(**pSer-150) cTnI by the western blotting.

Supplementary materials

Methods

Measurement of biological parameters

The systolic blood pressure and heart rate were measured with a tail-cuff method as previously described (1). Plasma cystatin C levels were determined with ELISA (Quantikine Mouse/Rat cystatin C Immunoassay, R&D Systems). Whole blood hemoglobin A1c was quantified with Mouse Hemoglobin A1c Assay Kit (Crystal Chem). Tissue ATP levels was measured with Invitrogen™ Molecular Probes™ ATP Determination Kit (ThermoFisher Scientific). Cardiac citrate synthase activity was studied with Citrate Synthase Activity Colorimetric Assay Kit (BioVision). Plasma levels of triiodothyronine (T3) and thyroxine (T4) were studied with ELISA (Mouse/Rat T3 and T4 Total ELISA, Calbiotech). Cardiac production of H_2O_2 was studied with Amplex® Red Hydrogen Peroxide/Peroxidase Assay Kit (ThermoFisher Scientific) as described elsewhere (2). Tissue levels of reduced glutathione (GSH) and oxidized glutathione (GSSG) were studied with GSH/GSSG Assay kit (Millipore Sigma). The levels of TGFβ1 and endothelin-1 in the heart lysate were studied with ELISA kits (Quantikine® Mouse/Rat/Porcine/ Canine TGFβ1 Immunoassay, R&D Systems; Quantikine® endothelin-1 immunoassay, R&D Systems).

Rac activity assay and Western blotting

The heart was homogenized in radioimmunoprecipitation assay (RIPA) buffer (50 mM Tris-HCl, pH 7.4, 150 mM NaCl, 50 mM β-glycerophosphate, 30 mM NaF, 2 mM EDTA, 2 mM EGTA, 30

mM $Na_4P_2O_7$, 2 mM Na_3VO_4, 1 % Triton X-100) containing protease inhibitors (cOmplete™, Roche). The homogenate was centrifuged at 1000g to pellet the nucleus and debris. Equal amounts of protein were pre-cleared with Pierce™ Glutathione Agarose (ThermoFisher Scientific) and incubated with p21-activated kinase (PAK)-p21 binding domain (PBD) Beads (Cytoskeleton) for 2 h at 4 ºC. The heat-dissociated proteins (40 µg/lane) were fractionated by SDS-PAGE (Mini-PROTEAN® TGX, Bio-Rad) and detected with Western blot by chemiluminescence (Supersignal™ West Pico PLUS, ThermoFisher Scientific). The antibody against Rac1 (Rabbit pAb; 21003; NewEast Biosciences) was used for Rac activity assay. The antibodies used for Western blot are as follows: ELMO1 (Rabbit mAb; 14457; Cell Signaling Technology), ELMO2 (Rabbit mAb; ab181234; Abcam), ELMO3 (Rabbit pAb; HPA021484; Atlas Antibodies), Dedicator of cytokinesis 180 (DOCK180; 4846; Rabbit mAb; Cell Signaling Technology), DOCK2 (Rabbit mAb; ab124838; Abcam), connexin43 (Rabbit pAb; 710700; ThermoFisher Scientific), Ser368-phosphorylated connexin 43 (Rabbit mAb; 52559; Cell Signaling Technology), dynamin-related protein 1 (DRP1; Rabbit mAb; 8570; Cell Signaling Technology), Ser616-phosphorylated DRP1 (Rabbit pAb; 3455; Cell Signaling Technology), mitochondrial fission factor (MFF; Rabbit mAb; 84580; Cell Signaling Technology), Ser146-MFF (Rabbit pAb; 49281; Cell Signaling Technology), mitofusin 2 (MFN2; Rabbit mAb; 9482; Cell Signaling Technology), 4-hydroxy-2-nonenal (Rabbit pAb; ab46545; Abcam), Small G protein signaling modulator 3 (SGSM3; Goat pAb; ABIN2559792; Antibodies Online), Caspase 3 (Rabbit mAb; 9665; Cell Signaling Technology), Cleaved Caspase 3 (Rabbit mAb; 9664; Cell Signaling Technology), Cardiac troponin I (Rabbit mAb; 13083; Cell Signaling Technology),

Ser150-phosphorylated cardiac troponin I (Rabbit pAb; p2010-150; PhosphoSolutions) and GAPDH (HRP-conjugated Rabbit mAb; 3683; Cell Signaling Technology).

HPLC analysis of the oxidation products of dihydroethidium

Superoxide levels were estimated by the HPLC quantification of the superoxide-specific dihydroethidium oxidation product, 2-dihydroxyethidium as previously described with some modifications (3). Briefly, heart slices were incubated in the phosphate-buffered saline (PBS) containing 10 μM dihydroethidium (Cayman) for 45 minutes at 37ºC in the dark. The tissue was washed in ice cold PBS and homogenized in ice cold PBS containing 0.1 % Triton X-100. The lysate supernatant (100 μl) was mixed with 100 μl of 0.2M HClO4 in methanol to allow protein precipitation on ice for 1 h, and centrifuged at 20,000g at 4ºC for 30 min. The supernatant (100 μl) was transferred to the tube containing 100 μl of 1M phosphate buffer PH2.6, and the resultant $KClO_4$ was precipitated by centrifugation at 20,000g at 4ºC for 15 min. The supernatant (100 μl) was transferred to the HPLC vial equipped with 200 μl conical glass insert for HPLC analysis using a Dionex Ultimate 3000 coupled to a Dionex Coularray Electrochemical Detector (Model 5600A) system (3). Separation was performed using a Kinetex 5 μm XB-C18 100 Å column 150 x 4.6 mm The chromatographic method was as follows: 0 min – 70%A-30%B, 10 min – 30%A-70%B, 10.1min – 100%B, 15.1 – 100%B, 15.2 min – 70%A-30%B, 20min – 70%A-30%B. Solvent A: 50 mM phosphate buffer pH 2.6 with 10% acetonitrile; Solvent B: 50 mM phosphate buffer pH 2.6 with 60% acetonitrile. This separation method resulted in retention times of 9.6 min for 2-hydroxyethidium and 9.8 min for ethidium.

Calpain Activity

Heart membranes were rapidly prepared using ice-cold buffer containing 6 mM Tris-base, pH 8.1, 0.2 mM EDTA, and 0.2 mM EGTA. Using equal protein aliquots, a portion of the membrane

preparations were incubated with 8 mM $CaCl_2$ at 37°C for 5-40 min, in the absence or presence of the calpain inhibitor E64d (4). Equal protein samples were denatured and separated by gradient SDS-PAGE for subsequent transfer to nitrocellulose. Blots were incubated in blocking solution containing BSA and stained with antibodies against cardiac α-spectrin (Rabbit pAb, Abcam). Anti-IgG-horseradish peroxidase conjugates were used for the secondary antibody step, and antigen staining and image development involved the chemiluminescence protocols using the GE Amersham AI600RGB imager. Immunostained bands were scanned at high resolution to determine integrated optical density with BIOQUANT software (R & M Biometrics).

Mitochondrial complex activity

The activity of cardiac mitochondrial complexes I, II, IV and V was studied with Abcam microplate assay kits (Complex I Enzyme Activity Assay Kit, ab109721; Complex II Enzyme Activity Assay Kit, ab109908; MitoTox™ Complex IV OXPHOS Activity Assay Kit ab109906; MitoTox™ Complex V OXPHOS Activity Assay Kit ab109907). The activity of cardiac mitochondrial complexes III was determined by studying the activity of decylubiquinol cytochrome c oxidoreductase (5).

Actin polymerization study

Total protein extracted from the heart was assayed by G-actin/F-actin In Vivo Assay Kit (Cytoskeleton).

Quantitative reverse transcription-PCR

Total RNA was extracted from different tissues and the mRNAs were assayed by quantitative reverse transcription-PCR as previously described (6). The primers and the probes used to measure the mRNAs are shown in **Supplemental Table 3**.

Histology and Immunofluorescence

After cutting the inferior vena cava, the left ventricle was punctured with a 23-gauge needle and perfused with PBS for 3 min and with 4 % paraformaldehyde for 5 min. Thereafter the tissues were dissected out and put in 4 % paraformaldehyde for at least 3 days. They were then paraffin embedded and sectioned. Sections were prepared by the Center for Gastrointestinal Biology and Diseases Histology Core and imaged on an Olympus BX61 microscope. Rabbit anti-neomycin phosphotransferase 2 antibody (Millipore Sigma), Alexa 488-conjugated goat anti-rabbit IgG antibody (ThermoFisher), rabbit anti-connexin43 antibody (ThermoFisher), Alexa 594-conjugated goat anti-rabbit IgG antibody (ThermoFisher) and DAPI (ThermoFisher) were used for the immunofluorescence. For electron microscopy, grids were prepared by the UNC Microscopy Services Laboratory and imaged on a Zeiss TEM 910 transmission electron microscope.

References

1. Krege JH, Hodgin JB, Hagaman JR and Smithies O. A noninvasive computerized tail-cuff system for measuring blood pressure in mice. *Hypertension*. 1995;25(5):1111-5.
2. Kuroda J, Ago T, Matsushima S, Zhai P, Schneider MD and Sadoshima J. NADPH oxidase 4 (Nox4) is a major source of oxidative stress in the failing heart. *Proc Natl Acad Sci U S A*. 2010;107(35):15565-70.
3. Zielonka J, Vasquez-Vivar J and Kalyanaraman B. Detection of 2-hydroxyethidium in cellular systems: a unique marker product of superoxide and hydroethidine. *Nat Protoc*. 2008;3(1):8-21.
4. Romine H, Rentschler KM, Smith K, Edwards A, Colvin C, Farizatto K, et al. Potential Alzheimer's Disease Therapeutics Among Weak Cysteine Protease Inhibitors Exhibit Mechanistic Differences Regarding Extent of Cathepsin B Up-Regulation and Ability to Block Calpain. *Eur Sci J*. 2017;13:38-59.
5. Spinazzi M, Casarin A, Pertegato V, Salviati L and Angelini C. Assessment of mitochondrial respiratory chain enzymatic activities on tissues and cultured cells. *Nat Protoc*. 2012;7(6):1235-46.
6. Kim HS, Lee G, John SW, Maeda N and Smithies O. Molecular phenotyping for analyzing subtle genetic effects in mice: application to an angiotensinogen gene titration. *Proc Natl Acad Sci U S A*. 2002;99(7):4602-7.

Supplemental Table 1. *P* values for two-way analysis of variance of the effects of ELMO1 genotype, diabetes mellitus and the interaction of ELMO1 genotype and diabetes on the parameters of echocardiography.

Parameters	*Elmo1* genotype	Diabetes	Interaction
LVEF	< 0.0001	< 0.0001	< 0.0001
LVPWd	0.0164	< 0.0001	< 0.0001
LVIDd	< 0.0001	0.0043	0.0219

LVEF. Left ventricular ejection fraction; LVPWd, Left ventricular posterior wall thickness in diastole; LVIDd, Left ventricular internal diameter in diastole. Overall, *Elmo1* genotype and diabetes significantly influence, and these factors mutually enhance the effects.

Supplemental Table 2. Primers for detection of *Elmo1* alleles with conventional PCR.

Allele		Sequence	Ampliconsize (bp)
*Elmo1*wt*	(Fwdprimer)	5'-TGCCTGAGTGCAAAACCTAC-3'	488
	(Revprimer)	5'-CTTCCAGTTTGGGAGGAATG-3'	
*Elmo1*L*	(Revprimer)	5'-TCCTCTCTGTAATGCACCAG-3'	574
*Elmo*H*	(Revprimer)	5'-ACAGTGGGAGTGGCATCTT-3'	570

Supplemental Table 3. Primers and probes for quantification of mRNA with real-time quantitative reverse transcription-PCR.

Gene Symbol		
Actb	(Fwd primer)	5'-AAGAGCTATGAGCTGCCTGA-3'
	(Rev primer)	5'-ACGGATGTCAACGTCACACT-3'
	(Probe)	5'-FAM-CACTATTGGCAACGAGCGGTTCCG-Tamra-3'
Edn1	(Fwd primer)	5'-TGCCACCTGGACATCATCTG-3'
	(Rev primer)	5'-ACGCTTGGACCTGGAAGAAC-3'
	(Probe)	5'-FAM-TCCCGAGCGCGTCGTACCGTATG-Tamra-3'
Elmo1	(Fwd primer)	5'-CCATTGAAGATCGTGTGATCTC-3'
	(Rev primer)	5'-CTTGTTTCTCATGGACCACC-3'
	(Probe)	5'-FAM-CAGGAGAGCATTCCATCATTGGCCG-Tamra-3'
Nox1	(Fwd primer)	5'-CTTTTATCGCTCCCAGCAGA-3'
	(Rev primer)	5'-CTCGCTTCCTCATCTGCAAT-3'
	(Probe)	5'-FAM-CGTGATTACCAAGGTTGTCATGCACCCA-Tamra-3'
Nox2	(Fwd primer)	5'-TGCCACCAGTCTGAAACTCA-3'
	(Rev primer)	5'-CAGCAGGTCTGCAAACCACT-3'
	(Probe)	5'-FAM-AGGCATGCGTGTCCCTGCACAGCCA-Tamra-3'
Nox4	(Fwd primer)	5'-AAGGAGCAAGGTCGCTTACA-3'
	(Rev primer)	5'-AGCAGCGGAATAAGGCCTGT-3'
	(Probe)	5'-FAM-TGCTGCCTGCTCTAATCAGGACCCA-Tamra-3'
Tgfb1	(Fwd primer)	5'-TGACGTCACTGGAGTTGTACGG-3'
	(Rev primer)	5'-GGTTCATGTCATGGATGGATGGTGC-3'
	(Probe)	5'-FAM-TTCAGCGCTCACGTCTCTTGTGACAG-Tamra-3'

Supplemental Figure legends

Supplemental Figure 1. Engulfment and cell motility protein 1 (ELMO1) and related protein levels. The number of animals studied is shown in each figure. Comparisons were done with one-way ANOVA. *, $P < 0.05$ vs. WT++ mice. NS, not significantly different among the 5 groups. **(A)** Relative ELMO1 protein levels in non-diabetic WT (WT++) and diabetic WT Akita (WTA+) hearts at age 16 weeks. **(B)** Relative dedicator of cytokinesis (DOCK) 180 protein levels, **(C)** relative DOCK2 protein levels, **(D)** Heart weight normalized by body weight (BW), and **(E)** relative Rac1 protein levels in Akita mice with 5 graded expressions of *Elmo1* at age 16 weeks.

Supplemental Figure 2. Physiological parameters in Akita mice with 5 graded expressions of *Elmo1* at age 16 weeks. Number of animals used are indicated in each figure. Dotted lines indicate non-diabetic WT levels. Comparisons were done with one-way ANOVA including the additional data set. NS, not significantly different among the 5 groups. **(A)** Plasma glucose. **(B)** Systolic blood pressure (BP). **(C)** Hemoglobin A1c (HbA1c) in the blood.

Supplemental Figure 3. Thyroid function in Akita mice with 5 graded expressions of *Elmo1* at age 16 weeks. Number of animals used are indicated in each figure. Dotted lines indicate non-diabetic WT levels. Comparisons were done with one-way ANOVA. NS, not significantly different among the 5 groups. **(A)** Plasma triiodothyronine (T3) levels. **(B)** Plasma thyroxine (T4) levels.

Supplemental Figure 4. Baseline values, histology, and cardiac functions with echocardiography and pressure-volume (PV) loop analysis in the non-diabetic mice with 5 graded expressions of *Elmo1* at age 16 weeks. The number of animals studied is shown in each figure. Comparisons were done with one-way ANOVA including the additional data set. NS, not significantly different among the 5 groups. **(A)** Heart weight normalized by body weight. **(B)** Systolic blood pressure (BP). **(C)** Heart rate. **(D)** Plasma glucose. **(E)** AZAN trichrome staining of the heart. Scale bar = 1 mm. **(F)** Ejection fraction of the left ventricles (LVEF). **(G)** Thickness of the left ventricular posterior wall in diastole (LVPWd). **(H)** Internal diameter of the left ventricle in diastole (LVIDd). **(I)** E-wave deceleration rate (EWDR) of the mitral flow. **(J)** The isovolumic relaxation time (IVRT) of the left ventricle. **(K)** Early tissue Doppler velocity (E'). **(L)** dP/dt Max. **(M)** End-systolic pressure-volume relationship (ESPVR). **(N)** End-diastolic pressure-volume relationship (EDPVR). **(O)** Tau Glantz.

Supplemental Figure 5. Renal histology and function in Akita mice with 5 graded expressions of *Elmo1* at age 16 weeks. Dotted line indicates non-diabetic WT levels. The number of animals studied is shown in each figure. Twenty glomeruli were analyzed in each animal for histology. Comparisons were done with one-way ANOVA including the additional data set. NS, not significantly different among the 5 groups. **(A)** Periodic acid-Schiff (PAS) staining with hematoxylin counter stain of the glomerulus. Scale bar = 50 μm. **(B)** Open capillary area. **(C)** PAS-positive area. **(D)** Plasma cystatin C levels.

Supplemental Figure 6. Parameters in the electrocardiogram. Eight mice in each group were examined. NS, not significantly different by one-way ANOVA. **(A)** PR intervals. **(B)** QRS complexes.

Supplemental Figure 7. Mitochondrial dysfunction and fragmentation. The number of animals studied is shown in each figure. Comparisons were done with one-way ANOVA including the additional data set. *, $P < 0.05$ vs. WTA+ mice by Tukey-Kramer Honestly Significant Differences test. NS, not significantly different among the 5 groups. **(A)** Mitochondrial complex IV activity. **(B)** Mitochondrial complex II activity. **(C)** Mitochondrial complex III activity. **(D)** Volume density of the mitochondria. **(E)** The median aspect ratio of mitochondria. **(F)** Relative amount of mitochondrial fission factor (MFF) protein. **(G)** Relative amount of dynamin-related protein 1 (DRP1). **(H)** Relative amount of mitofuscin-2 (MFN2) protein.

Supplemental Figure 8. Oxidative stress-related markers in the cardiac tissues. The number of animals studied is shown in each figure. Comparisons were done with one-way ANOVA including the additional data set. *, $P < 0.05$ vs. WTA+ mice by Tukey-Kramer Honestly Significant Differences test. NS, not significantly different among the 5 groups. **(A)** Reduced glutathione (GSH) content in the five groups of mice, six mice in each group. **(B)** Oxidized glutathione (GSSG) content in the five groups of mice, six mice in each group. **(C)** Individual fluorescence for 2-hydroxyethidium (2-OH-E^+) fluorescence (Red), Neomycin phosphotransferase II (Neo) immunoreactivity (Green), and nuclei attaining with DAPI (Blue) in

the heart of the *Elmo1*$^{L/+}$*Myh6-cre/Esr1Ins2*$^{Akita/+}$ mice intraperitoneally injected with low dose tamoxifen (20 mg/kg, 2 days). Tissue was chimeric with Neo-positive *Elmo1*$^{L/+}$ cardiomyocytes and Neo-negative *Elmo1*$^{H/+}$ cardiomyocytes. The merged image is presented in Figure 5D of the main text. The Neo-positive *Elmo1*$^{L/+}$ cardiomyocyte (†) has a lower 2-OH-E^{+} fluorescence than the Neo-negative *Elmo1*$^{H/+}$ cardiomyocyte (#). Scale bar = 10 μm. **(D)** Densitometric measures of the spectrin breakdown products (SBDP) before and after Ca^{2+} treatment were plotted on the left and the right, respectively. Values are expressed as % of αII-spectrin and plotted against mean *Elmo1* gene expression levels of LLA+ (30 %), WTA+ (100 %) and HHA+ (200 %). Two mice in each group. **(E)** mRNA levels of NADPH oxidase 1 gene (*Nox1).* **(F)** mRNA levels of NADPH oxidase 2 gene (*Nox2).* Amount of mRNA in each sample was normalized by mRNA of β-actin gene (*Actb*) and expressed relative to the mean values of WTA+ as 100 %. **(G)** Protein levels of TGFβ1. **(H)** Protein levels of endothelin-1.

Supplemental Figure 9. Effects of EHT1864 (a pan-Rac inhibitor) and VAS3947 (a pan NADPH oxidase inhibitor) and disruption of NADPH oxidase 4 gene (*Nox4*) (NOX4KO) in the HHA+ mice. Data of the untreated HHA+ mice are the same as those in the Supplemental Figure 4B, D and Supplemental Figure 5A-D. The number of animals studied is shown in each figure. Twenty glomeruli were analyzed in each animal for histology. Comparisons were done with one-way ANOVA including the additional data set. NS, not significantly different among the 4 groups. **(A)** Plasma glucose. **(B)** Systolic blood pressure (BP). **(C)** Periodic acid-Schiff

(PAS) staining with hematoxylin counter stain of the glomerulus. Scale bar = 50 μm. **(D)** Open capillary area. **(E)** PAS-positive area. **(F)** Plasma cystatin C levels.

Supplemental Figure 10. Echocardiography and pressure-volume loop study in the HHA+ mice subjected to the 4-week treatment with VAS3947 at age 16 weeks. Data of the untreated HHA+ mice are the same as those in the Figure 2A, F-M of the main text. Dotted lines indicate non-diabetic WT levels. The number of animals studied is shown in each figure. Comparisons were done with one-way ANOVA including the additional data set. *, $P < 0.05$ vs. untreated HHA+ mice by Tukey-Kramer Honestly Significant Differences test. **(A)** Representative M-mode echocardiography of the HHA+ mice treated with vehicle, EHT1864 or VAS3947, and of Nox4-null HHA+ mice. **(B)** E-wave deceleration rate (EWDR) of the mitral flow. **(C)** The isovolumic relaxation time (IVRT) of the left ventricle **(D)** Early tissue Doppler velocity (E'). **(E)** Representativepressure-volume loops. **(F)** dP/dt Max. **(G)** End-systolic pressure-volume relationship (ESPVR). **(H)** End-diastolic pressure-volume relationship (EDPVR). **(I)** Tau Glantz.

Supplemental Figure 11. Dissociation of the intercalated disc of heart muscle cells in the HHA+ mice treated with VAS3947. Data for the treated mice are presented together with those of HHA+ mice presented in the Figure 3A-C of the main text for comparison. The number of animals studied is shown in each figure. Comparisons were done with one-way ANOVA including the additional data set. *, $P < 0.05$ vs. untreated HHA+ mice by Tukey-Kramer Honestly Significant Differences test. **(A)** Representative images of the intercalated disc in the heart by the transmission electron microscopy. Arrows indicate the dissociation of intercalated

disc. Scale bar = 1 μm. **(B)** Frequency of the dissociation of intercalated disc. Percentage of discs with dissociated gap junctions per at least 30 discs. **(C)** Representative images for the immunofluorescence for connexin 43 (Cx43). The immunoreactivity for Cx43 was diminished in the intercalated discs in the HHA+ heart, which was restored by VAS3947. Arrows indicate intercalated discs. Scale bar = 10 μm.

Supplemental Figure 12. Mitochondrial dysfunction and fragmentation in the heart of HHA+ mice treated with VAS3947. The results from the six treated mice are presented together with those of HHA+ mice presented in the Figure 4A, B, E-G and Supplemental Figure 7D, E of the main text for comparison. Comparisons were done with one-way ANOVA including the additional data set. *, $P < 0.05$ vs. untreated HHA+ mice by Tukey-Kramer Honestly Significant Differences test. **(A)** ATP content. **(B)** Citrate synthase activity. **(C)** Representative transmission electron microscopy images of the mitochondria. The fragmentation was frequently observed in the Akita mice with high expression of *Elmo1,* which was restored by VAS3947. Arrows indicate mitochondria. Scale bar = 1 μm. **(D)** The number of the mitochondria. **(E)** Apparent sizes of the mitochondria. **(F)** Volume density of the mitochondria. **(G)** The median aspect ratio of mitochondria.

Supplemental Figure 13. Effects of VAS3947 on cleaved caspase 3 levels in the cardiac tissue of the HHA+ mice. The number of animals studied is shown in each figure. *, $P< 0.05$ vs. untreated HHA+ mice by one-way ANOVA. NS, not significantly different between the 2 groups. **(A)** Relative amount of total caspase 3. **(B)** Relative amount of cleaved caspase 3.

Supplemental Figure 14. Effects of EHT1864 and VAS3947 and disruption of *Nox4* (NOX4KO) on glutathione and protein levels in the cardiac tissue of the HHA+ mice. Data of the untreated HHA+ mice were taken from the previous experiments. The number of animals studied is shown in each figure. Comparisons were done with one-way ANOVA including the additional data set. *, $P < 0.05$ vs. untreated HHA+ mice by Tukey-Kramer Honestly Significant Differences test. NS, not significantly different among the 4 groups. **(A)** Total Rac protein. **(B)** Reduced glutathione (GSH) content. **(C)** Oxidized glutathione (GSSG) content. **(D)** Protein levels of TGFβ1. **(E)** Protein levels of endothelin-1.

Supplemental Figure 15. Filamentous (F-) and globular (G-) actin protein levels in diabetic hearts at age 16 weeks. F-actin/G-actin ratios in the diabetic heart having 5 ELMO1 genetic levels and the HHA+ heart treated with VAS3947. The number of animals studied is shown in each figure. Comparisons were done with one-way ANOVA. *, $P < 0.05$ vs WTA+ mice; **, $P < 0.05$ vs. untreated HHA+ mice by Tukey-Kramer Honestly Significant Differences test.

Supplemental Figure 16. Immunoblots for total and Ser150-phosphorylated cardiac troponin I (cTnI) using the whole heart lysate of Akita mice with graded ELMO1 expression. The number of animals studied is shown in each figure. Comparisons were done with one-way ANOVA. NS, not significantly different among the 5 groups. No difference was observed in **(A)** the total amount and in **(B)** Ser150-phosphorylated **(**pSer-150) cTnI by the

western blotting.